

Optical linewidth and field fluctuations in piezoelectric quantum wells

C. Bodin, R. André, J. Cibert, Le Si Dang, and D. Bellet

Laboratoire de Spectrométrie Physique, CNRS et Université J. Fourier, Boîte Postale 87, 38402 Saint Martin d'Hères, France

G. Feuillet and P. H. Jouneau

Département de Recherche Fondamentale sur la Matière Condensée, Commissariat à l'Energie Atomique, PSC-SP2M, Centre d'Etudes Nucleaires de Grenoble, 17 avenue des Martyrs, 38054 Grenoble Cedex 09, France

(Received 1 December 1994)

The photoluminescence linewidth in CdTe-based piezoelectric quantum wells increases with the quantum-well width: this demonstrates the contribution of fluctuations of the built-in field, which appear strongly correlated with the width of the x-ray-diffraction rocking curve. A more complete analysis of the Bragg peak in the reciprocal space allows us to propose a quantitative model.

I. INTRODUCTION

Strained semiconductor-compound heterostructures grown along a polar axis are known to incorporate a built-in field induced by the mismatch strain through piezoelectric effect.^{1,2} The component of this field parallel to the growth axis causes a spatial separation of electrons and holes confined in the quantum well (QW), greatly modifying the electronic properties of these heterostructures. In particular, the built-in field acts as a bias and enhances the sensitivity to any additional field: under an applied electric field one observes a linear Stark effect, as opposed to the quadratic one in a usual square QW;³ also the field due to photocreated carriers may partially cancel the built-in field, and this gives rise to significant optical nonlinearity at low excitation density,⁴ lower than the densities required for mechanisms⁵ which operate in square QW's. Both effects are thought to have potential applications in electrooptics and nonlinear optics. However, these structures are also very sensitive to less-controlled fields, such as surface fields related to band bending and Fermi energy pinning,⁶ or to field fluctuations due to residual strain or to electrically active defects. As a result, optical transitions are often severely broadened, and the optical quality very much depends on the structural quality of the whole heterostructure.^{7,8}

Here we show that the optical transitions in CdTe-based piezoelectric QW's are broadened by fluctuations of the built-in field. This results in a linear increase of the photoluminescence (PL) linewidth as a function of the QW width, contrarily to the decrease usually observed when the linewidth is due to fluctuations of the QW width, e.g., in (001) QW's. By comparing the PL line broadening and the x-ray-diffraction rocking curves on a series of samples, we establish that the field fluctuations are directly correlated to the structural quality of the buffer layer on which the QW's are grown. When the structural quality improves, the contributions of field fluctuations and of QW width fluctuations are of similar magnitude. All data on CdTe-Cd_{1-x}Zn_xTe and CdTe-Cd_{1-x}Mn_xTe structures are accounted for using a single linear relationship between the fluctuation of the built-in

field (measured on PL spectra) and the width of the x-ray-diffraction rocking curve. Finally a more complete analysis of the x-ray Bragg peak (identifying the roles of mosaic spread and of strain fluctuations using a high-resolution diffractometer) allows us to calculate the fluctuations of the built-in field due to strain fluctuations in good agreement with the experimental findings.

II. EXPERIMENTAL RESULTS

A. Samples

Samples under study are CdTe-Cd_{1-x}Zn_xTe and CdTe-Cd_{1-x}Mn_xTe QW's grown by molecular-beam epitaxy. The growth conditions and general optical properties have been described elsewhere.⁸ In all samples a thick buffer layer is grown first on a GaAs or Cd_{0.95}Zn_{0.05}Te substrate. Its thickness (2–4 μm) is far above the critical thickness, so that the buffer layer composition determines the lateral lattice parameter of the whole heterostructure: the strain in a CdTe QW grown on top of this buffer layer is imposed by the lattice mismatch $\delta a/a$ between CdTe and the buffer layer. Relaxation of the misfit strain between the buffer layer and the substrate occurs through the formation of structural defects. Growth conditions are chosen to favor the formation of a dense array of dislocations at the buffer/substrate interface; in particular, the use of vicinal surfaces and of well-chosen temperature sequences during the growth is determinant to avoid the formation and propagation of twins in the whole heterostructure. In samples of good structural quality relaxation indeed occurs through dislocations and microtwins which are restricted to the interface.

B. Photoluminescence and x-ray diffraction in Cd_{1-x}Zn_xTe-CdTe QW's

Figure 1(a) shows PL spectra of two CdTe-Cd_{0.84}Zn_{0.16}Te samples. It will be shown below that the structural quality of both samples is quite different due to slightly different growth conditions. Each sample in-

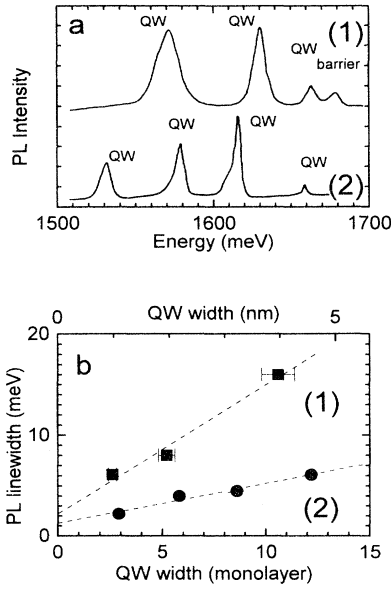


FIG. 1. Photoluminescence of two CdTe-Cd_{0.84}Zn_{0.16}Te samples (1 and 2), with several QW's on each sample. The plots are the (a) spectra, and (b) PL linewidth as a function of the QW thickness.

cludes several CdTe QW's of different widths, on a thick (111) Cd_{0.84}Zn_{0.16}Te buffer grown on a (001) GaAs substrate with a 4° miscut around $[\bar{1}10]$. As shown in Ref. 2 the redshift of the PL line is linear with the QW width, with a slope equal to the built-in field, 0.35 meV/Å in both samples. These spectra evidence a clear increase of the linewidth as the QW width increases. This is shown by Fig. 1(b), which displays the dependence of the PL linewidth on the QW thickness for the two samples of Fig. 1(a). On QW's with sharpest transitions one observes an extrinsic line 3–4 meV lower in energy than the intrinsic transition: this closely resembles PL spectra of (001) QW's, where the extrinsic line is, depending on the sample doping, either a donor-bound exciton or a two-electron X^- center.⁹ Then Fig. 1(b) displays the full width at half maximum of the intrinsic line. For strongly broadened transitions we took the overall linewidth. It is clear from Fig. 1(b) that the broadening increases linearly with the QW thickness, with a slope which depends on the sample under study.

In CdTe-Cd_{1-x}Zn_xTe QW's, such as those of Fig. 1, we have shown^{2,8} that electrons and holes are not or are barely confined in the QW (lattice mismatch is large and band offsets small, so that piezoelectric effect dominates over confinement effects). Then the electron level coincides with the conduction-band edge of the barrier on one side of the QW and the hole level with the valence-band edge of the barrier on the opposite side, so that the transition energy is given (if we neglect the exciton binding energy) by

$$E = E_G(\text{Cd}_{1-x}\text{Zn}_x\text{Te}) - qFL_w. \quad (1)$$

Differentiating we obtain the effect of a change of the

barrier gap $E_G(\text{Cd}_{1-x}\text{Zn}_x\text{Te})$, of the QW thickness L_w or of the built-in field F as

$$\delta E = \delta E_G(\text{Cd}_{1-x}\text{Zn}_x\text{Te}) - qF \times \delta L_w - qL_w \times \delta F. \quad (2)$$

In nonpiezoelectric QW's it is well established that the inhomogeneous width of the QW transitions is most often due to fluctuations of the QW thickness. The linewidth dependence is then $\Delta E = (dE/dL_w)\Delta L_w$, where the QW thickness fluctuation ΔL_w does not depend on L_w (but depends on growth conditions). Indeed ΔL_w is expected to be independent of L_w as soon as a stationary surface morphology is reached during the growth of the QW. This appears to be the case in GaAs-Ga_{1-x}Al_xAs QW's (Ref. 10) or CdTe-Cd_{1-x}Mn_xTe (Ref. 11) (001) QW's when broadening due to QW thickness fluctuations is dominant. A constant ΔL_w (independent of L_w) is also quite probable in the present case, since growth is performed on a vicinal surface and should occur through propagation of the existing steps. Inserting a constant ΔL_w into Eq. (2) we predict a linewidth independent of the QW thickness, in contradiction with Fig. 1(b). The same is true if we consider the direct effect of alloy fluctuations in Eq. (2). Hence Fig. 1(b) is a direct indication that transitions are broadened by fluctuations of the built-in field, with $\Delta E = qL_w\Delta F$. For the two samples of Fig. 1(b) we measure $\Delta F = 0.34 \pm 0.04$ and 0.11 ± 0.02 mV/Å, respectively.

A similar broadening was found in CdS-CdSe superlattices where the PL linewidth increases with the superlattice period and decreases upon screening of the built-in field by photoinjected carriers, which strongly suggests a broadening by field fluctuations.¹²

The field fluctuations ΔF may be due to charged defects, but also, through the piezoelectric effect, to strain fluctuations. While the former are difficult to evaluate, x-ray diffraction gives information on the latter. The width $\Delta\theta_{RC}$ of a rocking curve of the (444) Bragg peak of the buffer layer, using a single-crystal diffractometer, after deconvolution of the $K\alpha_1$ - $K\alpha_2$ doublet, including an apparatus contribution ≈ 0.5 to 1 mrad is $\Delta\theta_{RC} = 11$ mrad for the sample of Fig. 1 with $\Delta F = 0.34$ mV/Å, and $\Delta\theta_{RC} = 5$ mrad for the sample with $\Delta F = 0.11$ mV/Å, i.e., the same trend for x-ray diffraction as for field fluctuations. Figure 2 shows for a series of CdTe-Cd_{1-x}Zn_xTe

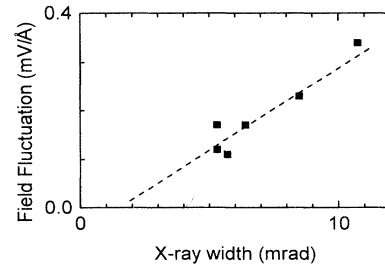


FIG. 2. Field fluctuation measured from the slope as in Fig. 1(b), as a function of the full width at half maximum of the (444) rocking curve. The samples have similar compositions (Cd_{1-x}Zn_xTe barriers with $x = 0.15$ – 0.18), but are grown under different conditions.

QW samples grown under different conditions, with $x = 0.15-0.18$, the field fluctuation ΔF measured as in Fig. 1(b), versus the full width of the (444) Bragg peak $\Delta\theta_{RC}$. In spite of some scattering we observe a strong correlation between the two sets of data, which is reasonably described by a linear fit $\Delta F \approx 30\Delta\theta_{RC}$, with the field in $\text{mV}/\text{\AA}$ and the width of the Bragg peak in rad. Indeed strain fluctuations (i.e., fluctuations of interatomic distance) are expected to broaden both the x-ray peak and the optical transition. We show below that the relationship between ΔF and $\Delta\theta_{RC}$ is not restricted to the present series of $\text{CdTe-Cd}_{1-x}\text{Zn}_x\text{Te}$ QW's with $x = 0.15-0.18$.

C. Experimental results on other samples

In order to compare results obtained on different kinds of samples, the relationship $\Delta F \approx 30\Delta\theta_{RC}$, obtained on the preceding series of $\text{CdTe-Cd}_{1-x}\text{Zn}_x\text{Te}$ (111) QW's with $x = 0.15-0.18$, i.e.,⁸ $F \approx 3 \text{ meV}/\text{\AA}$ and $\delta a/a \approx 10^{-2}$, is changed into

$$\frac{\Delta F}{F} \approx 0.1 \frac{\Delta\theta_{RC}}{\delta a/a}. \quad (3)$$

This relationship is dimensionless [$\Delta\theta_{RC}$ is the width of the (444) rocking curve, expressed in rad]. Moreover, the built-in field F is related to the lattice mismatch $\delta a/a$ through the piezoelectric coefficient e_{14} , and we expect the same coefficient to enter the relationship between the field fluctuation ΔF and the strain fluctuation (see below). We have shown elsewhere⁶ that in CdTe the piezoelectric effect is nonlinear: this dimensionless relationship allows us to compare samples where the lattice mismatch is different. Moreover, in the case of $\text{CdTe-Cd}_{1-x}\text{Zn}_x\text{Te}$ QW's Eqs. (1) and (2) show that (in the case where the linewidth is due to field fluctuations)

$$\frac{\Delta F}{F} = \frac{\Delta E}{E_G(\text{Cd}_{1-x}\text{Zn}_x\text{Te}) - E}, \quad (4)$$

where E is the PL energy of a particular QW, ΔE is the corresponding linewidth, and $E_G(\text{Cd}_{1-x}\text{Zn}_x\text{Te})$ is measured on the barrier: hence $\Delta F/F$ is measured directly on the PL spectrum, as the ratio of the width of each line to the redshift of the same line with respect to the barrier line. Variations of the exciton binding energy and Stokes shift are negligible. We shall first apply the same analysis to the case of $\text{CdTe-Cd}_{1-x}\text{Mn}_x\text{Te}$ structures grown along [111]. Typical spectra have been given in Refs. 6 and 8, where we have already stressed the influence of the structural quality of samples on the PL linewidth. In these samples definitely sharper x-ray rocking curves are recorded, typically 1–1.5 mrad: in this case we used double-crystal x-ray diffraction with an InSb monochromator. As a result of the better structural quality, the contribution of field fluctuations to the PL linewidth is smaller than in $\text{CdTe-Cd}_{1-x}\text{Zn}_x\text{Te}$ QW's, and the contribution of thickness fluctuations ΔL_w cannot be neglected. Figure 3 gives PL linewidths measured on two representative $\text{CdTe-Cd}_{1-x}\text{Mn}_x\text{Te}$ QW samples. For the first sample the linewidth decreases with the QW width, while it increases for the second one.

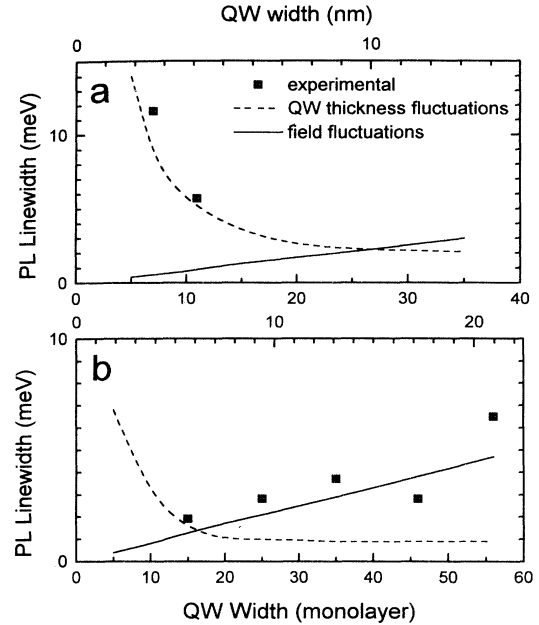


FIG. 3. PL linewidth for $\text{CdTe-Cd}_{1-x}\text{Mn}_x\text{Te}$ QW's, as a function of the QW thickness. Symbols are experimental results, lines are results of calculations: solid lines represent the effect of field fluctuations calculated for the width of the x-ray rocking curve, $\Delta\theta_{RC}$, measured on the same sample; dashed lines represent the effect of fluctuations of the QW thickness ΔL_w , which is the only adjustable parameter. Results are plotted for (a) $x = 0.23$, $\Delta\theta_{RC} = 1.0 \text{ mrad}$, and $\Delta L_w = 0.5 \text{ ML}$; and (b) $x = 0.19$, $\Delta\theta_{RC} = 1.2 \text{ mrad}$, and $\Delta L_w = 0.3 \text{ ML}$.

In the case of $\text{CdTe-Cd}_{1-x}\text{Mn}_x\text{Te}$ structures the lattice mismatch is smaller and band offsets are larger than in $\text{Cd}_{1-x}\text{Zn}_x\text{Te}$ QW's, so that the effect of quantum confinement is of the same order as that of the built-in field: Eq. (1) must be replaced by the result⁸ of a detailed calculation for $E(F, L_w)$. The contribution of field fluctuations was calculated as $\Delta E_F = (dE/dF)\Delta F$, where ΔF is obtained from Eq. (3); $\Delta\theta_{RC}$ is the width of the (444) rocking curve measured on the same sample through double-crystal diffraction, i.e., we use the same relationship as determined for $\text{Cd}_{1-x}\text{Zn}_x\text{Te}$ structures, without an adjustable parameter. The contribution of the QW width fluctuation was calculated as $\Delta E_L = (dE/dL_w)\Delta L_w$. Figure 3 illustrates that, depending on the heterostructure characteristics, the PL linewidth is due to field fluctuations, QW width fluctuations, or both. The only adjustable parameter is the QW thickness fluctuation ΔL_w , for which we find reasonable values (0.3–0.5 ML). In particular when the broadening due to field fluctuations dominates [Fig. 3(b)], the same relationship as for $\text{CdTe-Cd}_{1-x}\text{Zn}_x\text{Te}$ samples holds.

Finally the same analysis can be applied to other piezoelectric heterostructures. PL spectra from $\text{CdTe-Cd}_{1-x}\text{Zn}_x\text{Te}$ QW's grown along (112) exhibit the same linear redshift¹³ as a function of the QW width [Eq. (1)], and the same linear increase of the linewidth. On the

spectrum of Ref. 13 one measures $\Delta F/F \approx 0.07$, of the same order as $\Delta F/F \approx 0.04$ in Fig. 1. Hence (112) and well-controlled (111) CdTe-Cd_{1-x}Zn_xTe heterostructures appear to have similar structural quality, in spite of the greater difficulty to eliminate the twins in (111) growth.

The PL line shape depends not only on the excitonic density of states, but also on the dynamics of the excitons (spectral transfer). We have checked on many samples that the same behavior is observed for the PL linewidth and the PL excitation linewidth.⁷ Hence the PL linewidth is a good measure of the field fluctuations. Since field fluctuations probably occur at a rather large scale (as compared to the exciton Bohr radius) they are not averaged out (such an averaging over the exciton volume is well known for fluctuations of the QW width¹⁰ or for microscopic alloy fluctuations¹⁴).

D. Strain fluctuations and mosaic spread

The width of the Bragg peak in epilayers is due to strain fluctuations (changes in the interplane distance) but also to mosaic spread (orientation distribution of the diffracting planes). Both are expected to increase with the density of structural defects. However, local misorientations of the lattice do not alter the value of the built-in field.

The different contributions to the width of a conventional rocking curve in x-ray diffraction can be disentangled by recording an ω scan and a $\theta-2\theta$ scan (with thin slits in front of the detector, or in a diffractometer with a four-crystal monochromator and an analyzer): for such an experimental setup the instrumental function is nearly a δ function perpendicular to the diffraction plane (plane including the incident and diffracted wave vectors). One then can perform a map of the scattering intensity in reciprocal space.¹⁵ If the divergence of the beam is low enough, the width of the Bragg peak in an ω scan directly gives the fluctuation of the direction of the diffracting planes (which is generally attributed to the mosaic spread but also includes shear components of the strain tensor), i.e., $\Delta\omega = \Delta q_{\perp}/q$. If the monochromaticity is high enough, the width in a $\theta-2\theta$ scan is related to the distribution of the interplane distance, i.e., $\Delta\theta = (\Delta q_{\parallel}/q)\tan\theta$. In strained epilayers one often finds a contribution of mosaic spread larger than that of lattice spacing fluctuations.¹⁶ In this case the width of a conventional rocking curve (one performs a $\theta-2\theta$ scan, while keeping the slits in front of the detector widely opened), which combines both effects, is dominated by mosaic spread.

The two contributions were measured on a Cd_{0.6}Mn_{0.4}Te layer grown on a Cd_{0.95}Zn_{0.05}Te substrate, using a four-crystal monochromator and a two-crystal analyzer [both using (220) Ge diffraction]. The resolution is given by the beam divergence (around 12 arc sec) and the wavelength dispersion $\Delta\lambda/\lambda \approx 10^{-5}$. Figure 4 exhibits the isointensities of the (444) Bragg peak in reciprocal space (using Cu $K\alpha_1$ radiation, $\lambda = 0.1541$ nm, $\theta = 56^\circ$). The mosaic spread contribution is the largest one. We measure a full width at half maximum 170 arc sec in the ω scan (i.e., $\Delta q_{\perp}/q = 0.84 \times 10^{-3}$) and 120 arc sec in the $\theta-2\theta$ scan, (i.e., $\Delta q_{\parallel}/q = \Delta\theta/\tan\theta = 0.41 \times 10^{-3}$). On

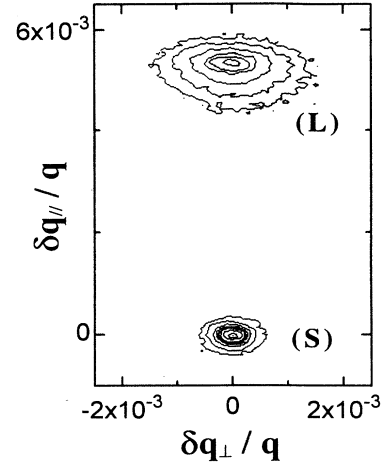


FIG. 4. Isointensities of the (444) Bragg peak of a Cd_{0.6}Mn_{0.4}Te layer (L) and its substrate (S). Full widths at half maximum are directly measured on the ω scan (170 arc sec for the layer and 11 arc sec for the substrate) and on the $\theta-2\theta$ scan (120 arc sec for the layer and 23 arc sec for the substrate). Plotted isointensities are 4, 10, 25, 50, 65, 85, 100, 400, 1200, and 2500 counts per second, with a maximum intensity 93 counts per second for the layer.

the same sample the width of the conventional rocking curve (i.e., without analyzer) is 240 arc sec ($\Delta\theta_{RC} = 1.2$ mrad).

To summarize, we have shown on a large series of CdTe-Cd_{1-x}Zn_xTe and CdTe-Cd_{1-x}Mn_xTe samples that the PL linewidth is due to, or includes, a contribution from fluctuations of the built-in field, with the relationship

$$\left[\frac{\Delta F}{F} \right]_{\text{exp}} \approx 0.1 \frac{\Delta\theta_{RC}}{\delta a/a} \quad (5)$$

between the field fluctuation and the width of the conventional (444) rocking curve. Moreover, on a CdTe-Cd_{1-x}Mn_xTe sample the detailed study of the (444) Bragg peak gives

$$\Delta\theta_{RC} \approx 2.9 \Delta q_{\parallel}/q, \quad (6)$$

hence

$$\left[\frac{\Delta F}{F} \right]_{\text{exp}} \approx 0.3 \frac{\Delta q_{\parallel}/q}{\delta a/a}. \quad (7)$$

III. DISCUSSION

In a strained (111) layer the piezoelectric field F and the displacement (with respect to unstrained CdTe) of a particular Bragg peak in reciprocal space can be expressed¹⁷ as a function of the strain tensor. The strain tensor itself can be calculated under the usual assumptions that stress components at the surface are zero [$\sigma_{33} = \sigma_{31} = \sigma_{32} = 0$, where (3) labels the growth axis, and (1) and (2) are two perpendicular axes within the growth

plane] and that the strain is isotropic within the growth plane ($\epsilon_{11} = \epsilon_{22} = \epsilon_{\parallel}$, $\epsilon_{12} = 0$), with $\epsilon_{\parallel} = \delta a/a$ in the case of a coherent QW.

One obtains

$$\epsilon_A = \epsilon_{xx} + \epsilon_{yy} + \epsilon_{zz} = \frac{12c_{44}}{c_{11} + 2c_{12} + 4c_{44}} \epsilon_{\parallel} \quad (8)$$

for the isotropic strain, and

$$\epsilon_{xy} = \epsilon_{yz} = \epsilon_{zx} = -\frac{c_{11} + 2c_{12}}{c_{11} + 2c_{12} + 4c_{44}} \epsilon_{\parallel} \quad (9)$$

for the trigonal strain components. The tetragonal strain components are zero. Here x , y , and z label the cubic axes.

The piezoelectric field is

$$\mathbf{F} = -\frac{2e_{14}}{\epsilon\epsilon_0} \begin{pmatrix} \epsilon_{yz} \\ \epsilon_{zx} \\ \epsilon_{xy} \end{pmatrix} = \frac{2e_{14}}{\epsilon\epsilon_0} \frac{c_{11} + 2c_{12}}{c_{11} + 2c_{12} + 4c_{44}} \epsilon_{\parallel} \begin{pmatrix} 1 \\ 1 \\ 1 \end{pmatrix}. \quad (10)$$

We will consider also the (444) Bragg peak. For unstrained CdTe,

$$\mathbf{q}_0 = 4/a_0 \begin{pmatrix} 1 \\ 1 \\ 1 \end{pmatrix},$$

with $a_0 = 6.481 \text{ \AA}$. For strained CdTe the variation $\mathbf{q} - \mathbf{q}_0$ of \mathbf{q} with respect to its unstrained value \mathbf{q}_0 is calculated using the strain tensor: the variation of the inter-plane distance corresponds to the longitudinal component of $\mathbf{q} - \mathbf{q}_0$ (here along the [111] direction), which writes

$$\frac{(\mathbf{q} - \mathbf{q}_0)_{\parallel}}{q_0} = \frac{(\mathbf{q} - \mathbf{q}_0) \cdot \mathbf{q}_0}{\mathbf{q}_0 \cdot \mathbf{q}_0} = \frac{1}{3}(\epsilon_{xx} + \epsilon_{yy} + \epsilon_{zz}) + \frac{2}{3}(\epsilon_{xy} + \epsilon_{yz} + \epsilon_{zx}). \quad (11)$$

The perpendicular variation of \mathbf{q} , which represents the rotation of the diffracting planes, contains shear strain components and the lattice misorientation ω (which would appear as antisymmetric components of the strain tensor):

$$\frac{(\mathbf{q} - \mathbf{q}_0)_{[\bar{1}\bar{1}2]}}{q_0} = \frac{1}{6}(2\epsilon_{zz} - \epsilon_{xx} - \epsilon_{yy}) - \frac{1}{3}\epsilon_{xy} + \frac{1}{6}\epsilon_{zx} + \frac{1}{6}\epsilon_{yz} + \omega. \quad (12)$$

The effect of small deviations of the strain components ($\delta\epsilon_{xx}, \dots$) and of the lattice misorientation can be derived from these expressions. For the field we are interested in the variation of the component normal to the QW,

$$\frac{\delta F}{F} = \frac{\delta \mathbf{F} \cdot \mathbf{F}}{\mathbf{F} \cdot \mathbf{F}} = \frac{\delta\epsilon_{xy} + \delta\epsilon_{yz} + \delta\epsilon_{zx}}{3\delta a/a} \frac{c_{11} + 2c_{12} + 4c_{44}}{c_{11} + 2c_{12}}. \quad (13)$$

For the Bragg peak we just differentiate Eq. (11):

$$\frac{\delta q_{\parallel}}{q} = \frac{1}{3}\delta(\epsilon_{xx} + \epsilon_{yy} + \epsilon_{zz}) + \frac{2}{3}(\delta\epsilon_{xy} + \delta\epsilon_{yz} + \delta\epsilon_{zx}). \quad (14)$$

The same combination of trigonal strain enters both Eqs. (13) and (14); however, the position of the Bragg peak depends also of the isotropic strain. This demonstrates that the field fluctuation and the width of the Bragg peak in a $\theta - 2\theta$ run are correlated, but the exact distribution of strain fluctuations and the correlations between the fluctuations of the various components of the strain tensor must be considered.

Our aim here is to check whether strain fluctuations in these samples have the right order of magnitude to account for the field fluctuations revealed by the width of QW photoluminescence lines. Hence we shall use the simplest hypothesis that the strain fluctuations can be described as fluctuations of the in-plane components of the strain tensor ($\epsilon_{11}, \epsilon_{22}, \epsilon_{12}$), the normal components of the stress tensor ($\sigma_{13}, \sigma_{23}, \sigma_{33}$) being zero. This corresponds to the idealized case of a dense array of structural defects in the vicinity of the buffer/substrate interface, the layer itself remaining free of defects and the surface free to relax. In addition to the fluctuation of the (symmetric) components of the strain tensor we must add fluctuations of the lattice misorientation (mosaic spread) due, e.g., to the screw components of misfit dislocations.

We shall simplify further this model by assuming that the strain imposed to the buffer layer remains isotropic in the layer plane; i.e., we have only fluctuations of ϵ_{\parallel} . Then it is straightforward to calculate

$$\frac{\Delta F}{F} = \frac{\Delta\epsilon_{\parallel}}{\delta a/a}, \quad (15)$$

and, for the (444) Bragg peak,

$$\frac{\Delta q_{\parallel}}{q} = 2 \frac{c_{11} + 2c_{12} - 2c_{44}}{c_{11} + 2c_{12} + 4c_{44}} \Delta\epsilon_{\parallel}, \quad (16)$$

while $\Delta q_{\perp}/q$ is restricted to the misorientation only.

Using $c_{11} = 5.35 \times 10^{10} \text{ N m}^{-2}$, $c_{12} = 3.68 \times 10^{10} \text{ N m}^{-2}$, and $c_{44} = 1.99 \times 10^{10} \text{ N m}^{-2}$, for CdTe, we obtain

$$\left[\frac{\Delta F}{F} \right]_{\text{calc}} = \frac{1}{2} \frac{c_{11} + 2c_{12} + 4c_{44}}{c_{11} + 2c_{12} - 2c_{44}} \frac{\Delta q_{\parallel}/q}{\delta a/a} = 1.2 \frac{\Delta q_{\parallel}/q}{\delta a/a}. \quad (17)$$

In spite of the crudeness of the model (we reduce the strain fluctuations to fluctuations of ϵ_{\parallel} only), this result compares favorably with the experimental result, though with a slightly smaller numerical factor in the experimental result.

In the actual layer strains probably do not remain isotropic within the layer plane: the measure of several Bragg peaks would give some information on the relative fluctuations of different components of the strain tensor. Moreover, defects propagate into the layer (threading dislocations, stacking faults, microtwins, twins, etc.): in this case strain fluctuations are not homogeneously distributed within the layer and decrease away from the interface. This effect of annihilation of the defects during growth was dramatically exemplified in a series of

different combinations of III-V semiconductors,¹⁸ where the density of threading dislocations was found to be inversely proportional to the layer thickness. This fact correlates well with the usual findings that the x-ray rocking-curve width decreases when the layer thickness increases. In thick layers (the intrinsic effect is negligible) with a finite density of threading defects, the width of the $\theta-2\theta$ profile, which integrates over the whole layer, combines at least two contributions: (i) the interplane distance varies across the layer, i.e., the mismatch strain is less relaxed close to the interface than near the surface; and (ii) at a given depth there are strain fluctuations due to the statistical distribution of defects. This broadening increases with the defect density, so that fluctuations close to the surface, where the QW's sit, are probably smaller than the average over the whole layer, which enters the x-ray profile. Hence the present x-ray-diffraction data overestimate strain fluctuations in the vicinity of the QW and the corresponding field fluctuations: indeed this improvement of the structural quality from the interface with the substrate to the layer surface probably accounts for the different numerical factors, 1.2 in the calculated relationship and 0.3 in the experimental one. A complete quantitative model should include a description of defect annihilation during the growth of the buffer layer and a measure of the distribution of strain

fluctuations (using surface-sensitive x-ray diffraction), and is out of the scope of this paper.

To conclude, in CdTe-based QW's grown along a polar axis (CdTe-Cd_{1-x}Zn_xTe along [111] and [211] and CdTe-Cd_{1-x}Mn_xTe along [111]) which incorporate a built-in field due to the piezoelectric effect, optical transitions are broadened by field fluctuations. These are strongly correlated to the structural quality of the buffer layer; as a result, field fluctuations in the top part of the buffer layer (measured optically) are found proportional to the width of the x-ray rocking curve. A quantitative model (although simplified) relates the field fluctuations to the fluctuations of the trigonal strain, measured in x-ray diffraction in a $\theta-2\theta$ scan. When compared to CdTe-Cd_{1-x}Zn_xTe, CdTe-Cd_{1-x}Mn_xTe structures not only exhibit a larger carrier confinement but also smaller relative fluctuations of the built-in field, correlated with the better structural quality of the epilayer.

ACKNOWLEDGMENTS

This work was partially completed within the CNRS-CEA Group Microstructures de Semiconducteurs II-VI. It has benefited from fruitful discussions and participation in the x-ray-diffraction measurements of P. Blanc, G. Dolino, and P. Fewster.

- ¹D. L. Smith and C. Mailhot, *Rev. Mod. Phys.* **62**, 173 (1990).
²R. André, C. Deshayes, J. Cibert, Le Si Dang, K. Saminadayar, and S. Tatarenko, *Phys. Rev. B* **42**, 11 392 (1990).
³E. A. Caridi, T. Y. Chang, K.W. Goossen, and L. F. Eastman, *Appl. Phys. Lett.* **56**, 659 (1990).
⁴K. W. Goossen, E. A. Caridi, T. Y. Chang, J. B. Stark, D. A. B. Miller, and R. A. Morgan, *Appl. Phys. Lett.* **56**, 715 (1990); I. Sela, D. E. Watkins, B. K. Laurich, D. L. Smith, S. Subbanna, and H. Kroemer, *Appl. Phys. Lett.* **58**, 684 (1991).
⁵S. Schmitt-Rink, D. S. Chemla, and D. A. B. Miller, *Phys. Rev. B* **32**, 6601 (1985).
⁶R. André, C. Bodin, J. Cibert, G. Feuillet, and Le Si Dang, *J. Phys. (France) IV* **5**, C-429 (1993).
⁷Le Si Dang, H. Okomura, C. Bodin, J. Cibert, G. Feuillet, and P. H. Jouneau, *Physica B* **185**, 490 (1993).
⁸J. Cibert, R. André, C. Bodin, G. Feuillet, P. H. Jouneau, and Le Si Dang, *Phys. Scr.* **49**, 487 (1993); J. Cibert, R. André, C. Bodin-Deshayes, G. Feuillet, Le Si Dang, K. Saminadayar, and S. Tatarenko, *J. Cryst. Growth* **117**, 424 (1992).
⁹K. Kheng, R.T. Cox, Y. Merle d'Aubigné, F. Bassani, K. Saminadayar, and S. Tararenko, *Phys. Rev. Lett.* **71**, 1752 (1993).
¹⁰C. Weisbuch, R. Dingle, P. M. Petroff, A. C. Gossard, and W. Wiegmann, *Appl. Phys. Lett.* **38**, 840 (1981); J. Singh, K. K.

- Bajaj, and S. Chaudhuri, *ibid.* **44**, 805 (1984); M. Tanaka and H. Sakaki, *J. Cryst. Growth* **81**, 153 (1987); V. Srinivas, J. Hryniewicz, Y. J. Chen, and C. E. C. Wood, *Phys. Rev. B* **46**, 10 193 (1992).
¹¹W. Grieshaber, C. Bodin, J. Cibert, J. Gaj, Y. Merle d'Aubigné, A. Wasieleski, and G. Feuillet, *Appl. Phys. Lett.* **65**, 1287 (1994).
¹²X. Chen, P. J. Parbrook, C. Trager-Cowan, B. Henderson, K. P. O'Donnell, M. P. Halsall, J. J. Davies, J. E. Nicholls, P. J. Wright, and B. Cockayne, *Semicond. Sci. Technol.* **5**, 997 (1990).
¹³F. Bassani, K. Kheng, M. Mamor, R. T. Cox, N. Magnéa, K. Saminadayar, and S. Tatarenko, *J. Cryst. Growth* **138**, 607 (1994).
¹⁴E. F. Schubert, E. O. Göbel, Y. Horikoshi, K. Ploog, and H. J. Queisser, *Phys. Rev. B* **30**, 813 (1984).
¹⁵P. F. Fewster, *J. Appl. Crystallogr.* **24**, 178 (1991).
¹⁶E.g., K. Kamigaki, H. Sakashita, H. Kato, M. Nakayama, N. Sano, and H. Terauchi, *Appl. Phys. Lett.* **49**, 1071 (1986).
¹⁷E. Anastassakis, *Phys. Rev. B* **46**, 4744 (1992).
¹⁸P. Sheldon, K. M. Jones, M. M. Al-Jassim, and B. G. Yacobi, *J. Appl. Phys.* **63**, 5609 (1988).